ELSEVIER

Biochimica et Biophysica Acta 1193 (1994) 316–322

BBA Biochimica et Biophysica Acta

Rapid computerized analysis of Na^+/H^+ exchange flux

Alastair J.M. Watson [1], Marshall H. Montrose *

Departments of Medicine and Physiology, Johns Hopkins University School of Medicine, Ross 930, 720 Rutland Ave., Baltimore, MD 21205, USA

Received 18 November 1993; revised 16 March 1994

Abstract

The regulation of intracellular pH (pH_i) is mediated by membrane transporters whose activity is directly controlled by pH_i. Therefore, transport rates must be compared at identical pH_i values in functional studies of these transporters. This is conventionally performed using scatter plots showing initial rates of proton flux versus intracellular pH. We present justification for determining proton flux over a wide range of pH_i, by digitally smoothing a pH_i trace and then directly taking the first derivative versus time of smoothed data. Compared to conventional least-squares analysis of initial rates, the derivative method generates much more information per experiment. Compared to other methods which fit pH_i traces to a defined equation prior to rate calculation, the new method does not require that the pH_i trace be well fit by any given mathematical function. The derivative technique is illustrated in an analysis of Na^+/H^+ exchange in Caco-2 cells. Intracellular pH is measured fluorometrically in cells loaded with BCECF (2′,7′-bis[2-carboxyethyl]-5-(and-6)carboxyfluorescein). To validate the analysis of Na^+/H^+ exchange over an extended time range, we demonstrate that cellular acidification with NH_4Cl does not change steady state Na^+ content. We find that proton flux rates analyzed by the derivative method are equivalent to initial rates measured by least-squares analysis.

Key words: pH; BCECF; Kinetics; Savitzky-Golay algorithm; Smoothing; Derivative; Caco-2 cell; (Intestine)

1. Introduction

Many membrane transporters responsible for regulating intracellular pH (pH_i) have rates of net proton flux which vary as a function of the absolute value of pH_i [1,2,10]. In the case of Na^+/H^+ exchange, the extreme sensitivity to pH_i has frequently been attributed to an intracellular allosteric proton binding site on the Na^+/H^+ exchange protein [1], although other explanations are also possible [14]. The regulation of acid/base transport by pH_i is obviously critical to the ability of the transporters to contribute to pH_i homeostasis. This property is also important for cellular regulation of acid/base transporters, because both second messenger agonists and environmental stimuli are known to alter the pH_i sensitivity of Na^+/H^+ exchange [9,12,16,17,22,23].

The regulation of acid/base transporters by pH_i imposes the requirement that fluxes may only be experimentally compared at identical pH_i values. Such comparisons are important for evaluation of transport mechanism, and for determination of altered transport properties caused by cellular regulation of transport [6,9,13,20–23]. Since it is difficult to attain precisely the same pH_i under different experimental conditions, the usual solutions to this requirement are either (1) present a scatter plot showing initial rates of proton flux versus pH_i (a single pH recovery trace generates a single data point) [7,11,13,20,21], (2) manually calculate rates at different pH_i values as tangents to the pH recovery trace [22], or (3) fit an entire pH recovery trace to a pre-defined mathematical equation (e.g., polynomial or exponential equations) so that pH recovery rates can be determined over a wide range of pH_i in a single trace [2,3,6,12,23]. The latter two methods are preferred because of the improved efficiency of data collection, and have been successfully applied in a number of cases [2,3,6,12,22,23]. However, calculation of rates as tangents is a slow manual procedure, and

* Corresponding author. Fax: +1 (410) 9559677.

[1] Present address: Department of Medicine, University of Manchester, Hope Hospital, Eccles Old Road, Salford, M6 8HD, UK

SSDI 0005-2736(94)00104-W

curve-fitting fits data to equations that may not match the appropriate transport model. Therefore, the 'best' equation to use will have to be determined empirically for each case.

In this report, a justification is presented for determining rates of proton flux over a wide range of pH_i, based in directly taking the first derivative of the pH_i recovery trace versus time. The advantage of such an approach is that curve fitting is eliminated while the maximum amount of information is collected from a single pH_i recovery trace. In this report, we have used measurements of pH_i and cellular Na^+ content in Caco-2 cells to evaluate and justify this method for measuring Na^+/H^+ exchange over an extended range of pH_i. These cells were derived from a human colon carcinoma [5], and have been shown previously to activate only basolateral Na^+/H^+ exchange during recovery from an intracellular acid load [20].

2. Materials and methods

Cell culture. Caco-2 cells [5] were grown in a 5% CO_2/ 95% air humidified incubator at 37°C in Dulbecco's modified Eagles medium (Hazelton Biologics, St. Lexena, KS) supplemented with 25 mM $NaHCO_3$, 10 mM Hepes, 50 IU/ml streptomycin, 50 μg/ml penicillin, 1% non-essential amino acids and 10% fetal bovine serum. For flourometry, cells were seeded onto polycarbonate filters coated with rat-tail collagen (PVPF, 5 μm pore size, Nucleopore, Pleasanton, CA) and studied 10–24 days after seeding (7–21 days post-confluency).

Intracellular pH. Intracellular pH (pH_i) was measured with BCECF (2',7'-bis[2-carboxyethyl]-5-(and-6)carboxyfluorescein) as described [20]. Briefly, cells on filters were loaded with BCECF by incubation for 60 to 90 min with 6.25 μM of the acetoxymethyl ester (Molecular Probes, OR) at room temperature in Na^+ medium (containing in mM: 130 Na^+Cl, 5 KCl, 2 $CaCl_2$, 1 $MgSO_4$, 1 $NaPO_4^{2-}$, 25 glucose, 20 Hepes, titrated to pH 7.4 at 23°C with Na^+OH^+ (pH 7.3 at 37°C). Fluorescence was measured in a SLM-Aminco spectrofluorometer (SPF-500C, SLM, Urbana, IL) equipped with a stirred cuvette, thermostated to 37°C. The cuvette was perfused to allow changes of extracellular medium during experimentation. The flow rate was 12.5 ml/min (5 cuvette volumes per min). Excitation wavelengths for BCECF were alternated between 500 ± 1 and 440 ± 1 nm while emission was monitored at 530 ± 20 nm. Autofluorescence was determined daily from a filter seeded with cells but not loaded with dye. Autofluorescence-corrected ratio values were measured every 3 s during the experiment. Ratios of 500/440 fluorescence were used to calculate pH_i as described previously [19,20] (ratio units are linearly correlated with pH_i from pH 6.4–7.5, data not shown). Cells were acidified by transient perfusion for 3–20 min with Na^+ medium supplemented with 30 mM NH_4Cl (NH_4-prepulse). When cells were exposed to medium without sodium, TMA^+ medium was used (in which tetramethylammonium replaced sodium mol : mol).

Cellular ion content. Total cellular Na^+ was determined by flame photometry as described previously [15,21]. Results are presented as nmol ion/mg cellular protein. Protein was determined by the Bradford procedure [4] using γ-globulin as standard.

3. Results

Caco-2 cells can be acidified by transient exposure to NH_4Cl (see Materials and methods; [20]). Caco-2 cells recover from this acid load by activating a basolateral amiloride-sensitive Na^+/H^+ exchanger which returns intracellular pH (pH_i) to starting values [20]. As shown in Fig. 1, after the Na^+-dependent pH recovery to resting pH_i, neither addition of 1 mM amiloride nor removal of sodium from the perfusate causes acidification. Consistent with previous results [20], this implies that Caco-2 Na^+/H^+ exchange is inactive at resting pH_i, and suggests that no other transporters contribute to pH_i regulation under these conditions. This suggests that the pH_i recovery trace can be used to specifically measure Na^+/H^+ exchange activity over a wide range of pH_i.

As shown in Fig. 1, the pH_i recovery trace gradually diminishes in slope as pH_i alkalinizes. This has been attributed to the presence of an internal proton modifier site which regulates net Na^+/H^+ exchange [1], but could also be partially due to diminishing Na^+ gradient (driving force) during the flux interval. To test the latter possibility, experiments measured the effect of pH_i recovery on cellular Na^+ content. The combination of NH_4Cl-prepulse and one hour preincubation in Na^+-free (TMA^+) medium depleted cells of Na^+ (shown in the filled triangles of Fig. 2, time zero). When Na^+-depleted cells were exposed to Na^+ medium (Fig. 2, filled triangles), cells required 5 min to return Na^+ to resting levels. This implies that pH_i recovery of Na^+-depleted cells is accompanied by changes in the Na^+ gradient. Since we wished to avoid this complication, experiments also measured the effects of NH_4Cl-prepulse with brief (5 min) exposure to Na^+-free (TMA^+) medium. As shown in the open symbols of Fig. 2, this protocol had no significant effect on steady state Na^+ content of Caco-2 cells. Therefore, all subsequent experiments utilized the latter protocol for generation of an NH_4-prepulse acid load, and brief stabilization of this acid load in TMA^+ medium, prior to inititation of Na^+/H^+ exchange activity by exposure to

Na^+ medium. Using these conditions, changes in cellular Na^+ will not complicate Na^+/H^+ exchange kinetics during an extended pH_i recovery time-course.

3.1. Application of the derivative method in Na^+-replete cells

Fig. 3 illustrates the analysis of pH_i recovery kinetics over a wide range of pH_i. In Fig. 3, the Na^+-free perfusate (containing tetramethylammonium:TMA^+ medium) was replaced with Na^+ medium at time zero to activate Na^+/H^+ exchange. Fig. 3A shows individual data points of a pH_i recovery after cells were

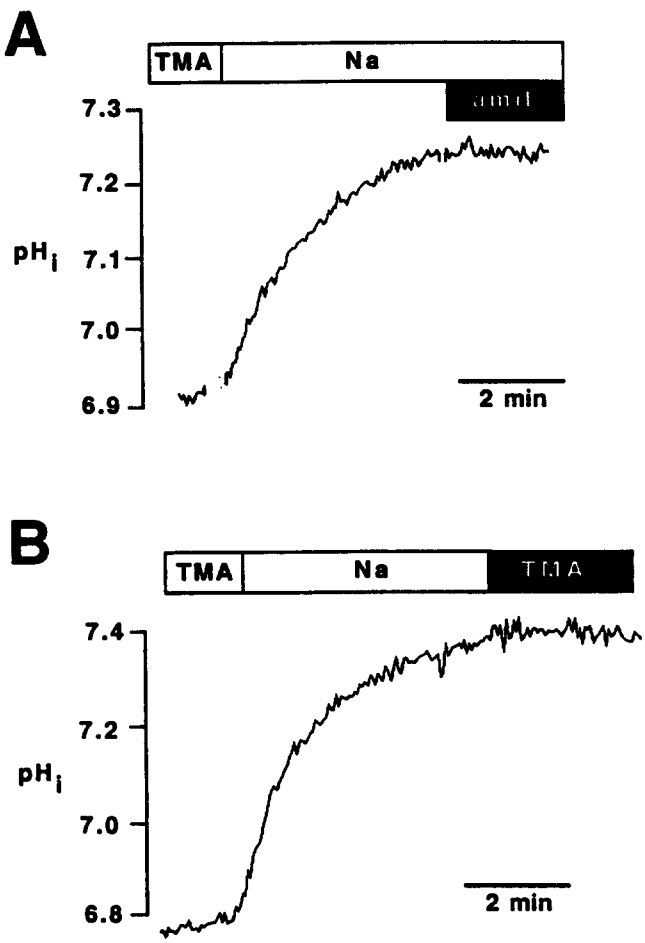

Fig. 1. Recovery of pH_i from an acid load in Caco-2 cells. Na^+/H^+ exchange is the only transporter mediating pH_i alkalinization and is inactive at resting pH_i. Caco-2 cells were loaded with BCECF, perfused 20 min with Na^+ medium plus 30 mM NH_4Cl, then cells were briefly (1–2 min) perfused in TMA^+ medium to allow stable acidification. Cells were then perfused with Na^+ medium to initiate pH_i recovery from the acid load via Na^+/H^+ exchange [20]. Intracellular pH was measured as (500/440) ratios of fluorescence in response to alternating excitation wavelengths and converted to intracellular pH via a nigericin/high K^+ calibration curve (see Materials and methods [20]). (A) At the indicated times, cells were exposed to Na^+ medium supplemented with 1 mM amiloride. (B) After cells alkalined to resting pH_i, the perfusate was returned to the Na^+-free (TMA^+) medium.

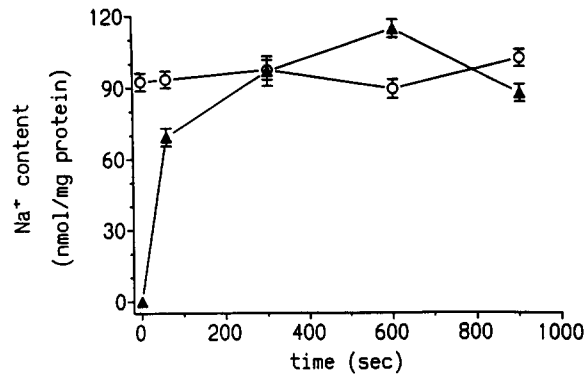

Fig. 2. Cellular Na^+ content of Caco-2 cells during Na^+-dependent pH_i recovery. Caco-2 cells were incubated for 60 min at 37°C in Na^+ (○) or TMA^+ (▲) medium and acidified by addition of 30 mM NH_4Cl for the final 20 min of incubation. All cells were then washed three times with TMA^+ medium (roughly 2 min) and Na^+ medium was added at time zero. Total cellular Na^+ content was measured by flame photometry at the times indicated. Results were normalized to cellular protein. Results are presented as the mean of three experiments ± S.E.

acidified with an NH_4Cl prepulse, presented in the original 500/440 ratio units output by the fluorometer. Data points in Fig. 3B show the result of calculating the first derivative of these raw data points values using the Savitzky-Golay algorithm [18]. As shown in Fig. 3B, the first derivative has high values (rapid pH_i recovery) at times corresponding to low pH_i, and diminishing values at high pH_i. However, extraction of reliable data was difficult because of noise in the data.

To reduce noise in the data, the original ratio trace was subjected to digital smoothing (also via a Savitzky-Golay algorithm) [18]. The available version of the algorithm (Inplot, SLM) applied a cubic convolute to sets of 7 data points during the smoothing operation, to determine a 'smoothed' value at the central point. As described [18], the weighting values in the convolute matrix are fixed, and the algorithm scans through the pH recovery trace in sets of 7 data points to generate a smoothed pH trace. This is a very mild smoothing algorithm and single passes cannot adequately eliminate noise in the typical pH data set (data not shown). Therefore, we have applied multiple smoothing passes. The solid line in Fig. 3A shows the result of 20 smoothing passes applied to the individual data points in 3A. As addressed earlier [18], the effect of multiple smoothing passes is mathematically equivalent to performing a single smoothing pass using a convolute which analyzes more data points. As shown, smoothing can be achieved without significant loss of fidelity from the original data. Since too much smoothing will blunt rapid transients (dotted line illustrates 160 smoothing passes), it is recommended that the original data be directly compared with the smoothed data (as done in Fig. 3A).

The first order derivatives of the smoothed data sets were then calculated as before and are presented in Fig. 3B as lines. As shown, the blunting of transients by the smoothing operation introduces a bias into the data (values are lower than predicted) until the maximum derivative is obtained. Independent of the amount of smoothing, at time points after the maximum, smoothing does not bias data. For this reason, only values after the maximum were included in further analysis. Control experiments showed that taking the derivative prior to smoothing of the data gave identical results (data not shown). Because smoothing blunts rapid transients, it is recommended to use the minimum number of smoothing passes required to adequately eliminate data scatter.

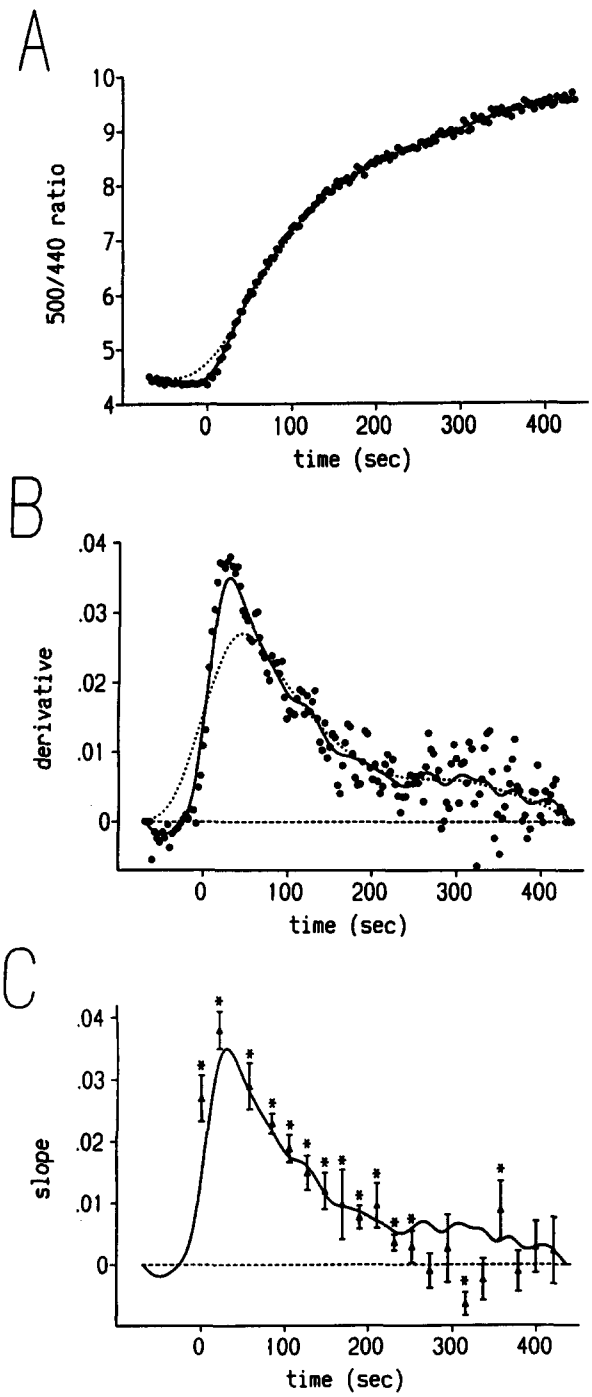

3.2. Comparison of the derivative method with linear least-squares fits

To demonstrate equivalence between the least-squares method and the derivative method, two experimental procedures were applied. We first generated least-squares fits along the entire pH_i recovery trace shown in Fig. 1A, using 7 data points for each fit (each spanning 21 s without overlap of data). The slopes are presented as data points in Fig. 1C, overlayed with the line depicting the derivative values after 20 smoothing passes. As shown, the data from the two methods are indistinguishable at time points after the maximum derivative is attained. The only possible discrepancy is at time points > 250 s, when the majority of the least-squares fits are not significantly different from a slope of zero, yet the smoothed derivative reports a small but positive slope. At these time points, Fig. 1A demonstrates that pH_i is still alkalinizing, supporting the derivative data but not the least-squares fit data. Therefore, use of smoothing helps the derivative method resolve slow rates of pH_i recovery which are poorly resolved with linear least-squares analysis.

A second method was used to compare between initial rates generated by least-squares versus the derivative method applied to an entire pH_i recovery trace. Five experiments were analyzed by both techniques. The starting acidification was varied intention-

Fig. 3. Intracellular pH recovery of Caco-2 cells from an acid load: illustation of the derivative method. Caco-2 cells were loaded with BCECF, and pH_i measured precisely as described in the legend to Fig. 1. (A) 500/440 ratio data. Prior to time zero, Caco-2 cells were perfused with TMA^+ medium. Starting at time zero cells were perfused with Na^+ medium to activate Na^+/H^+ exchange. Fluorescence ratio data were collected at 3-s intervals and are presented as individual points in the figure. The solid and dotted lines show experimental data after 20 or 160 passes of digital smoothing, respectively, using a Savitzky-Golay algorithm [18]. (B) The first order derivative of the smoothed data from A was calculated using a Savitzky-Golay alogorithm [18]. Each data point corresponds to the derivative calculated from the raw ratio data at the equivalent time point in A. The horizontal dashed line indicates zero net proton flux. The solid and dotted lines present derivatives calculated from ratio data which was smoothed 20 or 160 times, respectively. (C) The 20-times smoothed derivative in B is reproduced as a line in C. Data points are slopes determined from the raw data shown in A, calculated using a linear least-squares fit of seven data points at each indicated time point. Error bars are standard deviations of the slope (provided in the output from the linear least-squares fit). Asterisks indicate linear least-squares values which are significantly different from zero ($P < 0.05$) by two-tailed t-test.

ally so that the results from the two methods would overlap for direct comparison. Least-squares analysis of initial rates were performed as described previously [20]. For analysis by the derivative method, (fluorescence ratio) data sets were smoothed and then the first order derivative calculated (as shown above). All further calculations were then performed in a spreadsheet (Lotus 123, version 3). Each derivative value was multiplied by the appropriate conversion factor to obtain units of pH per s *, and then multiplied by the buffering capacity of the Caco-2 cells to obtain net proton flux in units of μM proton per s. Each buffering capacity value was calculated for the pH_i value at which the derivative was calculated, using a linear equation which was previously shown to relate buffering capacity to pH_i over the range $pH_i = 7.5–6.8$ [20]. A second linear equation was fit to the buffering capacity data from pH_i 6.8–6.5, because of the increased amount of buffering at these pH_i values [20]. It should be noted that these calculations would be impractical by hand, since each pH_i recovery is composed of roughly one hundred data points.

Results from this analysis are shown in Fig. 4. Smaller symbols present individual data points calculated from the derivative method, and larger symbols present data from the least-squares analysis. Each symbol shape represents data collected from a single pH_i recovery of Caco-2 cells. Both data sets demonstrate the reproducibility of the data and the sensitivity of Na^+/H^+ exchange to pH_i. The variability in individual pH_i recoveries is at the level expected from previous work [20]. As shown by the overlap between the two data sets, the new methodology can effectively supplement initial rate data.

3.3. Non-Michaelis-Menten activation of Na^+/H^+ exchange fluxes by intracellular protons

Previous work used initial rates of Caco-2 Na^+/H^+ exchange to identify sigmoidicity in the activation of net Na^+/H^+ exchange by intracellular protons [20]. Thus to be useful, the derivative method must also be sensitive enough to detect positive cooperativity in the data. Therefore, proton flux rates were calculated in 7 experiments analyzed by the derivative method and plotted versus intracellular $[H^+]$ in Fig. 5. The sigmoid curve presented in the figure is identical to that used previously [20] to fit the data generated from inital rates of Caco-2 Na^+/H^+ exchange. As shown, the compiled derivative data set cannot be readily extrapolated through the origin unless significant positive cooperativity is present in the curve fit. This data set demonstrates the positive cooperativity most clearly as an apparent 'set point' at which net flux can no longer be distinguised from zero (30 nM H^+ = pH 7.52). Previous analyses have emphasized determination of this set

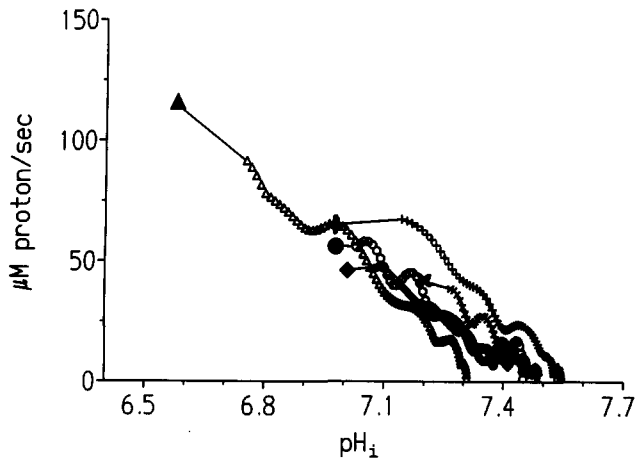

Fig. 4. Comparison within the same experiments, between Na^+-dependent H^+ efflux rate calculated by the derivative method and the least-squares fit of initial rates. BCECF fluorescence ratio data from five pH_i recovery experiments performed as in Fig. 1 were smoothed (10–20 passes), and the first order derivative calculated as shown in Fig. 3. The acid load was varied by changing the preincubation time in NH_4Cl (5–20 min). Rates of proton flux were calculated as the product of the pH_i change per unit time and the buffering capacity of cells at the same pH_i. Each symbol shape presents data from a separate pH_i recovery. Each derivative datum was used to calculate net proton flux (μM proton per s) (small symbols). The large symbols present the initial rate of proton efflux calculated from the same experiments. Initial rates were calculated using a linear least-squares fit of the data over approximately the first 30 s of Na^+-dependent pH_i recovery.

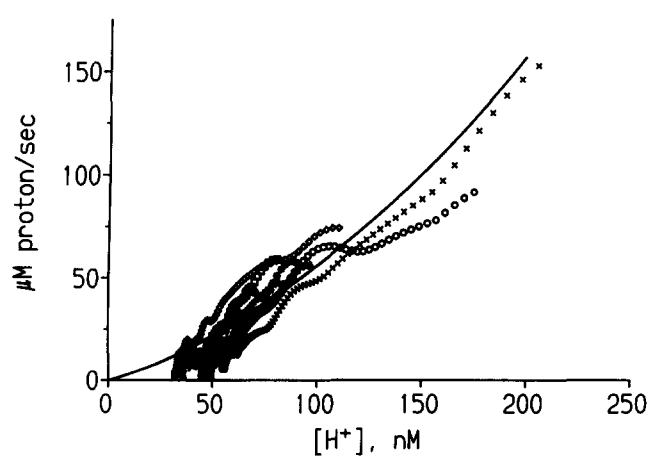

Fig. 5. Demonstration of sigmoidal activation kinetics in compiled results from the derivative method. Seven pH_i recovery experiments were performed, and proton efflux rates calculated, as described in Fig. 4. The pH scale was then converted to $[H^+]$ and results plotted. Each symbol shape presents data from a separate pH_i recovery. The line is reproduced from a previous publication [20] and was used previously to fit scatter plots of data generated from initial rate calculations of pH recovery in the same cells.

* This factor is calculated from the standard calibration line of 500/440 ratio versus pH_i. The inverse of the slope (in our case 0.1593 pH units/ratio unit) is the desired conversion factor.

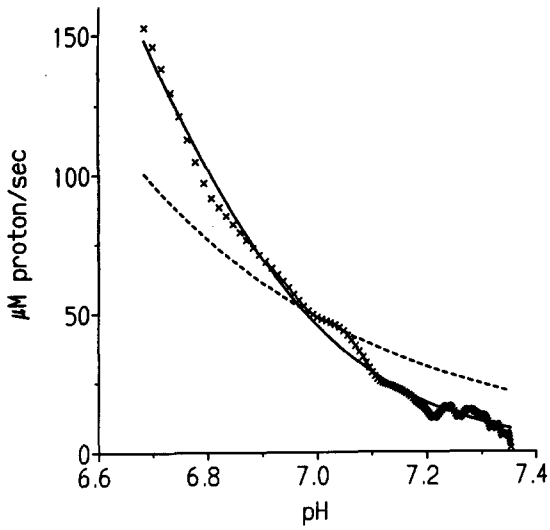

Fig. 6. Demonstration of sigmoidal activation kinetics in results from a single experimental run analyzed by the derivative method. A single experimental run analyzed by the derivative method is reproduced from Fig. 5 (X). The data was fit to a form of the Hill equation (see text) in which the Hill coefficient was either fixed at one (dotted line), or in which the Hill coefficient was allowed to vary (solid line). As shown, positive cooperativity in proton binding was required to generate a reasonable fit of the data to the equation.

point as a major characteristic of Na^+/H^+ exchange properties [10,16,22,23].

We also compared the ability of different equations to fit a single experimental run in the presence versus absence of positive cooperativity (i.e., Hill coefficient > 1 or $= 1$, respectively). The data points in Fig. 6 are from a single pH_i recovery trace analyzed by the derivative method. Data were fit with a nonlinear least-squares fit to the Hill equation (in the precisely equivalent form of a three-parameter logistic equation: designed to analyze data as the negative log of proton concentration (i.e. $pH = -\log [H^+]$)). In this equation,

$$V = \frac{V_{max}}{1 + (10^K/10^X)^{-N}}$$

in which proton flux (V) is a function of intracellular pH (X), and the computer determines the maximum proton flux rate (V_{max}), the pH which causes half maximal transport (K), and the Hill coefficient (N). The solid line in Fig. 6 is the fit resulting when V_{max}, K and N are allowed to vary independently. The resulting Hill coefficient was 2.25, and the fit was good ($r^2 = 0.991$). In contrast, the dashed line is the best fit ($r^2 = 0.764$) when V_{max} and K were allowed to vary independently, but N was fixed at one (no positive cooperativity; enforced Michaelis-Menten kinetics). As shown, positive cooperativity in the data was strongly suggested by the poor fit when $N = 1$. The results in Figs. 5 and 6 provide two techniques which demonstrate non Michaelis-Menten kinetics in results from the derivative method.

4. Discussion

Our goal was to establish a simple method for analysis of proton flux data which was appropriate for a wide variety of transport mechanisms and which took advantage of the large amount of information available within an extended time-course of pH change. Similar methods which have been successfully applied previously have either required curve fitting to a mathematical formula that was not based in a transport model, or manual calculation of tangent slopes [2,3,6,12,22,23]. A major goal was to overcome these limitations.

We have used the Caco-2 model to establish such a method because under our conditions (1) only a single transport system (Na^+/H^+ exchange) mediates pH_i recovery from an acid load, and (2) the Na^+ gradient is constant during extended time-courses of pH_i recovery. The latter point is important because in contrast to studies of initial rate kinetics, changes in starting conditions (e.g., ion gradients) may occur during extended experimental intervals. Therefore, to accept any method which studies kinetics of proton transport over extended time and pH_i ranges, it is essential to determine which of the substrates of the studied transport system are changing during the experiment. For example, since Na^+/H^+ exchange is observed experimentally after the removal and replacement of medium Na^+ for varying time intervals, it is predicted that intracellular Na^+ concentration may vary significantly during pH_i recovery mediated by Na^+/H^+ exchange. Thus, prior to the application of techniques which evaluate extended time-courses of Na^+/H^+ exchange activity, it was important to establish conditions such that intracellular Na^+ was constant during the experiment. A related control was run by Takaichi et al. [22], in which they tested for changes in Na/H exchange kinetics when sodium loading was varied.

The derivative method takes advantage of some commonly available methods for data analysis. The Savitzky-Golay algorithm calculates derivatives at each time point based on analysis of a fixed number of data points surrounding the time point under study [18]. The algorithm is available in standard software which controls SLM and Perkin Elmer fluorometers, from graphics software such as InPlot, or it can be written based on the original description [18]. A related algorithm [18] was used for smoothing of data. In our case, this was performed using the SLM software supplied by the fluorometer manufacturer, but the method is also commonly available (e.g., InPlot).

The derivative method has some limitations. The major limitation is that rates of proton flux are under-

estimated at the times directly after activation of transport (e.g., after return of Na^+ to activate Na^+/H^+ exchange). However, it is simple to define the point at which the derivative values become reliable (at the peak of the derivative values), and we suggest that the derivative method be used as a supplement, not replacement, for initial rate calculations. In 12 pH_i recoveries, the maximum value of the smoothed derivative was attained 8–15 data points after the initiation of pH_i recovery (i.e., reintroduction of Na^+ to the perfusate). This corresponds (in the SPF-500C) to 24–45 s in each experiment which cannot be analyzed by the derivative method due to the nature of the algorithm. Instruments allowing faster rates of data collection would reduce this 'dead time' proportionally.

A second limitation of the derivative method is that data traces must be smoothed prior to extracting values. As shown in Fig. 3B, smoothing further restricts the collection of data away from the time when transport is activated. However, smoothing allows the reliable extraction of data even when rates of pH_i recovery are troublesome to analyze by least-squares analysis (Fig. 3C). The amount of smoothing required will vary depending on the quality of data, but as shown in Fig. 3B even intentional 'over-smoothing' does not change the quality of data (after the maximum derivative value is obtained). This implies that the method is robust when applied correctly.

A third limitation of the method is that it is best applied when only a single transport mechanism is active during the measured pH_i change. This method measures the sum of all transport which contributes to pH_i regulation under the utilized conditions. While the derivative method is appropriate for cells (such as Caco-2) which use only one transporter for pH regulation, other methods are more appropriate for analysis of complex systems involving multiple transporters, and/or significant acidification from metabolism [3,6,8,12].

In summary, we have applied an easy method allowing rapid analysis of proton flux rates. The derivative method does not require knowledge of transport models, and does not make any assumptions about the mechanism of transport. When used to analyze Na^+/H^+ exchange kinetics, values generated by the derivative method compare favorably with those from linear least-squares fits along the curve (Fig. 3), or initial rate calculations generated in the same cell line (Figs. 4 and 5) [20]. The method also preserves the non-Michaelis-Menten of transport defined earlier [20], as demonstrated in two separate analyses (Figs. 5 and 6). Thus results from the derivative method are directly comparable to more conventional least-squares analysis of initial rates, but provide roughly 100-fold more data per experiment.

Acknowledgements

We gratefully acknowledge Dr. Arie Moran whose suggestion prompted this study, Joseph Covington who performed the cell culture, and Dr. Diego Restrepo for helpful discussion. This work was supported by a grant from the National Institutes of Health (DK 42457).

References

[1] Aronson, P.S., Nee, J. and Suhm, M.A. (1982) Nature 299, 161–163.
[2] Boron, W.F., McCormick, W.C. and Roos, A. (1979) Am. J. Physiol. 237, C185–C193.
[3] Boyarsky, G., Ganz, M.B., Cragoe, E.J. and Boron, W.F. (1990) Proc. Natl. Acad. Sci. USA 87, 5921–5924.
[4] Bradford, M.M. (1976) Anal. Biochem. 72, 248–254.
[5] Fogh, J., Fogh, J.M. and Orfeo, T. (1977) J. Natl. Cancer Inst. 59, 223–226.
[6] Ganz, M.B., Boyarsky, G., Sterzel, R.B. and Boron, W.F. (1989) Nature 337, 648–651.
[7] Grinstein, S., Cohen, S. and Rothstein, A. (1984) J. Gen. Physiol. 83, 341–369.
[8] Montrose, M.H. and Murer, H. (1990) Am. J. Physiol. 259, C110–C120.
[9] Grinstein, S., Rothstein, A. and Cohen, S. (1985) J. Gen. Physiol. 85, 765–787.
[10] Grinstein, S. and Rothstein, A. (1986) J. Membr. Biol. 90, 1–12.
[11] Tse, C.-M., Levine, S.A., Yun, C.H.Y., Brant, S.R., Pouyssegur, J., Montrose, M.H. and Donowitz, M. (1993) Proc. Natl. Acad. Sci. USA, 90, 9110–9114.
[12] Sjaastad, M.D., Wenzl, E. and Machen, T.E. (1992) Am. J. Physiol. 262, C164–C170.
[13] Helmle-Kolb, C., Montrose, M.H., Stange, G. and Murer, H. (1990) Pfluegers Arch. 415, 461–470.
[14] Montrose, M.H. and Murer, H. (1988) in Na^+/H^+ Exchange (Grinstein, S., ed.), pp. 57–76, CRC Press, Boca Raton, FL.
[15] Montrose, M.H. and Murer, H. (1987) J. Membr. Biol. 97, 63–78.
[16] Moolenar, W.H., Tsien, R.Y., Van der Saag, P.T. and Laat, S.W. (1983) Nature 304, 645–646.
[17] Rood, R.E., Emmer, E., Wesolek, J., McCullen, J., Hussain, Z., Cohen, M., Braithwaite, R.S., Murer, H., Sharp, G.W.G. and Donowitz, M. (1988) J. Clin. Invest. 82, 1091–1097.
[18] Savitzky, A. and Golay, M.J.E. (1964) Anal. Chem. 36, 1627–1939.
[19] Thomas, J.A., Bushbaum, R.N., Zimiak, A. and Racker, E. (1979) Biochemistry 18, 2230–2238.
[20] Watson A.J.M., Levine, S., Donowitz, M. and Montrose, M.H. (1991) Am. J. Physiol. 261, G229–G238.
[21] Watson A.J.M., Levine, S., Donowitz, M. and Montrose, M.H. (1992) J. Biol. Chem. 267, 956–962.
[22] Takaichi, K., Balkovetz, D.F., Meir, E.V. and Warnock, D.G. (1993) Am. J. Physiol. 264, C944–C950.
[23] Livne, A.A. and Aharonivitz, O. (1992) Biochim. Biophys. Acta 1135, 13–18.